

# Variation in foliar nitrogen and albedo in response to nitrogen fertilization and elevated CO<sub>2</sub>

Haley F. Wicklein · Scott V. Ollinger · Mary E. Martin ·  
David Y. Hollinger · Lucie C. Lepine · Michelle C. Day ·  
Megan K. Bartlett · Andrew D. Richardson · Richard J. Norby

Received: 21 January 2011 / Accepted: 15 January 2012 / Published online: 1 February 2012  
© Springer-Verlag 2012

**Abstract** Foliar nitrogen has been shown to be positively correlated with midsummer canopy albedo and canopy near infrared (NIR) reflectance over a broad range of plant functional types (e.g., forests, grasslands, and agricultural lands). To date, the mechanism(s) driving the nitrogen-albedo relationship have not been established, and it is unknown whether factors affecting nitrogen availability will also influence albedo. To address these questions, we examined variation in foliar nitrogen in relation to leaf spectral properties, leaf mass per unit area, and leaf water content for three deciduous species subjected to either nitrogen (Harvard Forest, MA, and Oak Ridge, TN) or CO<sub>2</sub>

Communicated by Gerardo Avalos.

H. F. Wicklein (✉) · S. V. Ollinger · M. E. Martin ·  
L. C. Lepine · M. C. Day  
Complex Systems Research Center, Morse Hall,  
Institute for the Study of Earth, Oceans, and Space,  
University of New Hampshire, 8 College Rd,  
Durham, NH 03824, USA  
e-mail: hwicklein@abermail.sr.unh.edu; hwicklein@gmail.com

D. Y. Hollinger  
Northern Research Station, US Department of Agriculture  
Forest Service, Durham, NH 03824, USA

M. K. Bartlett  
Department of Environmental Science, Policy, and Management,  
University of California, Berkeley, CA 94720, USA

A. D. Richardson  
Department of Organismic and Evolutionary Biology,  
Harvard University Herbarium, Harvard University,  
22 Divinity Avenue, Cambridge, MA 02138, USA

R. J. Norby  
Environmental Sciences Division,  
Oak Ridge National Laboratory, Oak Ridge,  
TN 37831, USA

fertilization (Oak Ridge, TN). At Oak Ridge, we also obtained canopy reflectance data from the airborne visible/infrared imaging spectrometer (AVIRIS) to examine whether canopy-level spectral responses were consistent with leaf-level results. At the leaf level, results showed no differences in reflectance or transmittance between CO<sub>2</sub> or nitrogen treatments, despite significant changes in foliar nitrogen. Contrary to our expectations, there was a significant, but negative, relationship between foliar nitrogen and leaf albedo, a relationship that held for both full spectrum leaf albedo as well as leaf albedo in the NIR region alone. In contrast, remote sensing data indicated an increase in canopy NIR reflectance with nitrogen fertilization. Collectively, these results suggest that altered nitrogen availability can affect canopy albedo, albeit by mechanisms that involve canopy-level processes rather than changes in leaf-level reflectance.

**Keywords** Albedo · Nitrogen · Leaf structure · Nitrogen fertilization · Free air CO<sub>2</sub> enrichment

## Introduction

The relationship between mass-based foliar nitrogen (N) and leaf-level photosynthetic capacity has been globally documented across a wide range of plant species (Field and Mooney 1986; Evans 1989; Reich et al. 1997, 1999; Wright et al. 2004), and a similar trend has been observed at the canopy level for boreal and temperate forests (Ollinger et al. 2008). Recently, Ollinger et al. (2008) and Hollinger et al. (2010) demonstrated that both of these variables are also significantly and positively correlated with full spectrum canopy albedo. Given the importance of even small changes in albedo on surface heat exchange, the

occurrence of an N effect on albedo would bear interesting and potentially important consequences for climate. However, resolving underlying mechanisms of the N–albedo relationship will be important because different mechanisms can carry different implications for a response to altered N availability.

Sources of variation in vegetation albedo occur at scales ranging from internal leaf structures to tree crowns and whole plant canopies (Ollinger 2011). At the leaf level, reflectance is dominated by photosynthetic pigments in the visible part of the spectrum (400–700 nm), leaf structure in the near infrared (NIR, 700–1,350 nm), and water content in the mid-infrared (Mid IR, 1,350–2,500 nm) (Gates et al. 1965; Slaton et al. 2001; Jacquemoud et al. 2009). At the stem and canopy level, the number of scattering or absorbing surfaces that photons encounter is further influenced by structural traits such as shoot architecture, leaf angle distribution, and crown geometry (e.g., Chen and Cihlar 1995; Asner 1998; Rautiainen et al. 2004). The greatest variation in reflectance at both leaf and canopy levels often occurs in the NIR region because there are few, if any, compounds that absorb NIR radiation (Gates et al. 1965; Sánchez and Canton 1999; Ollinger 2011). Therefore, if structural changes that occur within or between leaves covary with foliar N, they could explain the nature of the canopy-level N–albedo relationship.

Hollinger et al. (2010) hypothesized that the association between leaf N concentration ( $N_{\text{mass}}$ ) and canopy albedo may be due to covariation between N-containing photosynthetic enzymes and internal leaf structures necessary to support different rates of photosynthesis. Particularly important are changes in the ratio of the mesophyll surface area exposed to intercellular air spaces to the area of the leaf ( $A_{\text{mes}}/A$ ), which has been shown to be positively correlated with both photosynthetic rates (Nobel et al. 1975; Longstreth et al. 1985) and NIR reflectance (Slaton et al. 2001). Given the different refractive indices of hydrated mesophyll cells and the intercellular airspace (Woolley 1971; Gausman et al. 1974), a higher  $A_{\text{mes}}/A$  value should lead to more opportunities for radiation scattering, and correspondingly higher reflectance.

The objectives of this study were (1) to test the hypothesis that the canopy level association between foliar  $N_{\text{mass}}$  and canopy albedo stems from a similar relationship occurring at the leaf level, and (2) to determine whether two forms of disturbance that are known to affect N availability—N fertilization and elevated CO<sub>2</sub>—can also influence leaf and canopy albedo. We measured leaf reflectance and transmittance, as well as leaf chemical and structural traits (N concentration, leaf mass per area, equivalent water thickness, and water content), for three deciduous species in the eastern US that have been subjected to either long-term N or CO<sub>2</sub> fertilization. Data from multiple free air CO<sub>2</sub>

enrichment (FACE) sites have shown that elevated CO<sub>2</sub> leads to an increase in leaf mass per unit area (LMA, Norby et al. 2003) and the consequent dilution of foliar N due to the accumulation of carbohydrates (Oren et al. 2001; Ellsworth et al. 2004; Norby and Iversen 2006). Therefore, if the canopy albedo–N relationship is driven by changes at the leaf level, we would expect to see higher leaf-level leaf albedo in plots subjected to N fertilization and lower leaf albedo in plots exposed to elevated CO<sub>2</sub>, relative to those receiving ambient CO<sub>2</sub> and N deposition. We also obtained canopy reflectance data from the airborne visible/infrared imaging spectrometer (AVIRIS) to examine whether canopy-level spectral responses were consistent with leaf-level results.

## Materials and methods

### Study sites

We measured spectral, chemical, and structural characteristics of leaf samples from two sites in the eastern US: Harvard Forest, Petersham, MA (42.5°N, 72°W) and Oak Ridge National Laboratory, Roane County, TN (35.9°N, 84.3°W). These sites were chosen because they contain deciduous tree species relevant to our objectives and because they allowed us to examine the spectral response of leaves to N fertilization and elevated CO<sub>2</sub>, both of which represent important environmental change agents that are known to alter leaf  $N_{\text{mass}}$ .

### Harvard forest, MA

Harvard Forest (HF) is located in Central Massachusetts and has been a long-term ecological research site since 1988. A chronic N fertilization experiment was established at HF in 1988 (Magill et al. 2004). Two stands were chosen for N additions: a mixed hardwood stand that regenerated naturally after a clearcut around 1945, and an even-aged red pine (*Pinus resinosa* Aiton) stand that was heavily disturbed by an ice storm in December of 2008, and not used in this study. In each stand, four plots were established: control (no added N), low N (additions of 50 kg N ha<sup>-1</sup> year<sup>-1</sup>), low N plus sulfur (not included in this study), and high N (additions of 150 kg N ha<sup>-1</sup> year<sup>-1</sup>). Each plot measures 30 × 30 m. Additions of ammonium nitrate (NH<sub>4</sub>NO<sub>3</sub>) began in 1988 and are distributed over six equal applications during the growing season (May–September). Mean annual precipitation at HF is 1,100 mm, distributed evenly throughout the year. Ambient N deposition averages 8 kg N ha<sup>-1</sup> year<sup>-1</sup> (Ollinger et al. 1993). The dominant soil types are stony- to sandy-loams formed from glacial till. Elevation is 385 m above sea level.

### Oak Ridge National Environmental Research Park, TN

The free air CO<sub>2</sub> enrichment (FACE) facility at the Oak Ridge National Laboratory (ORNL) Environmental Research Park is located in a sweetgum (*Liquidambar styraciflua* L.) monoculture that was established in 1988 (Norby et al. 2001). In 1996, five 25-m-diameter plots were established: two with FACE apparatus emitting elevated CO<sub>2</sub>, two with FACE apparatus but ambient CO<sub>2</sub>, and one with no FACE apparatus. Exposure to elevated CO<sub>2</sub> began in the spring of 1998. Average daytime CO<sub>2</sub> concentration for 2009 was maintained at approximately 565 ppm for the enriched plots and 401 ppm for the ambient plots (Riggs et al. 2009). In 2004, an N fertilization experiment was initialized in a sweetgum stand located approximately 150 m from the FACE site and planted at the same time. An 85 m × 50 m area was fertilized in a block pattern, with each block containing two control plots and two fertilized plots (both 12 × 16 m). The fertilized plots received 200 kg N ha<sup>-1</sup> year<sup>-1</sup>, applied as urea each year before leaf out (Iversen and Norby 2008). Mean annual temperature at Oak Ridge is 14°C, and mean annual precipitation is 1,371 mm, distributed evenly throughout the year. Ambient N deposition averages between 10 and 15 kg N ha<sup>-1</sup> year<sup>-1</sup> (Johnson et al. 2004). The dominant soil type is an Aquic Hapludult, a silty clay loam.

### Data collection and analysis

#### Field sampling: Harvard Forest

At HF, sampling of foliage from the control and treated hardwood plots was conducted between 20 and 23 July 2009. Within each plot, five red maple and seven black oak trees were randomly selected and sampled. Green leaves were collected from the top, middle, and bottom of the canopy using a 12-gauge shotgun. Sample collection heights were determined using a digital hypsometer (Haglöf Vertex). Leaves were placed in plastic Ziploc bags and stored on ice until analysis, which was carried out within 36 h of collection.

#### Field sampling: Oak Ridge National Environmental Research Park

At ORNL, field sampling was conducted between 28 and 30 July 2009. Using a slingshot canopy sampler (N-fertilized site) or tower climbing with pole pruners (FACE site), we collected green leaves from the top, middle, and bottom of the canopy. Heights were determined using either a digital hypsometer (Haglöf Vertex) or measuring tapes deployed by climbers. Within each CO<sub>2</sub> fertilization treat-

ment (ambient and elevated CO<sub>2</sub>), we sampled ten sweetgum trees. From each N-fertilized plot, we collected 12 upper canopy and 12 lower canopy samples. The adjacent FACE ambient CO<sub>2</sub> plots were used as the control treatment for the N-fertilized samples in statistical analysis. In all cases, leaves were placed in plastic Ziploc bags and stored on ice until analysis.

### Collection of field spectra

We measured hemispherical reflectance and transmittance spectra for healthy leaves from each individual using a portable spectrometer (ASD FieldSpec 3; analytical Spectral Devices, Boulder, CO, USA) connected to an integrating sphere with an 8° near-normal incidence port to capture both diffuse and specular reflectance (SphereOptics, Concord, NH, USA) and a halogen bulb light source. The ASD spectrophotometer was used in conjunction with an integrating sphere, which holds leaf samples in a fixed position and is intended to eliminate angular effects by creating perfectly diffuse radiation. It measures reflectance from 350 to 2,500 nm, in 1-nm intervals. For each sample, measurements were taken for a single leaf and stacks of two, four, and eight leaves. Reflectance and transmittance spectra of leaf stacks were taken to create optically dense layers of leaf tissue, in order to examine how reflectance varies as a function of the total thickness of the leaf material present. Each leaf spectrum was determined as the average of 50 individual scans. The spectra were corrected for dark current, and a white reference standard was measured prior to each set of reflectance or transmittance measurements of one growing stack of leaves. For reflectance measurements, both the sample and the reference standard were mounted on the sphere and their positions were switched between two successive scans. Spectral reflectance was then calculated as the ratio of the value obtained from the sample to the value obtained from the reference.

To calculate full spectrum (FULL, 400–2,500 nm) spectrally weighted optical values, each reflectance or transmittance spectra was weighted by the solar spectrum energy (ASTM G173-03 Reference Spectra received by a 37° tilted equator-facing surface through an air mass of 1.5, derived from SMARTS v. 2.9.2; Gueymard 2004) to obtain a value representing the reflected (denoted as  $\alpha_{\text{FULL}}$ ) or transmitted (denoted as  $\tau_{\text{FULL}}$ ) energy as a proportion of incident. These values approximate albedo values measured using broadband radiometric instruments. For visible ( $\alpha_{\text{vis}}$  or  $\tau_{\text{vis}}$ , 400–700 nm), NIR ( $\alpha_{\text{nir}}$  or  $\tau_{\text{nir}}$ , 700–1,300 nm), and Mid IR ( $\alpha_{\text{midir}}$  or  $\tau_{\text{midir}}$ , 1,350–2,500 nm) portions of the spectrum, the solar-weighted reflectance and transmittance values were calculated by following the same process, but using only wavelengths from the regions of interest.

### Leaf chemical and structural analysis

After spectral measurements were obtained, two circular disks ( $2.035 \text{ cm}^2$  area) were removed from each leaf and weighed. Leaf disks were then oven-dried at  $70^\circ\text{C}$  for at least 72 h and reweighed to determine water content (% leaf fresh weight), equivalent water thickness (EWT, g water per  $\text{cm}^2$  leaf), and LMA (g leaf per  $\text{m}^2$  leaf).

The remaining leaf sample was then dried at  $70^\circ\text{C}$ , ground using a Wiley mill, and passed through a 1-mm mesh screen. Prior to N concentration analysis, the ground samples were dried for 24 h at  $70^\circ\text{C}$ . We measured mass-based foliar N concentration ( $N_{\text{mass}}$ , g of N per 100 g of dry leaf matter) using a Costech Elemental Analyzer. We determined N per unit leaf area ( $N_{\text{area}}$ ) by multiplying  $N_{\text{mass}}$  by the LMA of the sample ( $N_{\text{area}} = N_{\text{mass}} \times \text{LMA}$ ).

### Aircraft remote sensing

For the ORNL site, high spectral resolution remote sensing images were acquired from NASA's AVIRIS (Airborne Visible/InfraRed Imaging Spectrometer) instrument within 10 days of our field sampling. AVIRIS measures upwelling radiation in 224 contiguous optical bands from 400 to 2,500 nm with a spectral resolution of 10 nm. AVIRIS was flown on an ER-2 at an altitude of 5,500 m giving a spatial resolution of 4.6 m. The image dataset was orthorectified by NASA JPL, and atmospherically corrected with ImSpec LLC's Atmospheric Correction Now (ACORN) v.6, transforming data from calibrated sensor radiance to apparent surface reflectance. After removing strong water adsorption bands that contained no usable data, we determined canopy reflectance for each treatment by averaging reflectance values within each waveband for pixels falling within each of the plots. Due to the spatial resolution of the image and the size of the treatment plots, we were able to obtain 36 pixels in the ambient  $\text{CO}_2$  plot, 12 pixels in the elevated  $\text{CO}_2$  plot, and 24 pixels in the N-fertilized.

### Statistical analysis

Summary statistics (means and standard error) were computed for all optical properties and leaf traits. The significances of the mean differences between treatments were determined by analysis of variance (ANOVA), with pairwise comparisons tested using Tukey's 'Honest Significant Difference' method. Regression analysis was used to determine relationships between optical properties and leaf traits. For multiple regressions the adjusted  $r^2$  was considered instead of  $r^2$  because this statistic penalizes the model for an increased number of parameters, thereby decreasing the likelihood of overfitting.

The Shapiro-Wilk statistic was used to test for normality in all models, and where needed variables were power-transformed to correct for skew. Single leaf  $\alpha_{\text{FULL}}$  and  $\alpha_{\text{nir}}$  were non-normal due to a small number of outliers (determined by  $1.5 \times$  interquartile range). Statistical tests were performed with and without the outliers, and, because the resulting explained variances were similar, outliers were removed to follow assumptions of normality in linear regression models. All statistical analysis was completed using the software R, v.2.8.1 (R Foundation for Statistical Computing, 2008). Reported results are for single leaves unless otherwise specified.

## Results

### Treatment differences

Across all species and sites,  $N_{\text{mass}}$  was higher in the high N treatment than in the low N and control treatments, which were not significantly different from each other ( $P < 0.001$ ; Fig. 1a–c). For red maple and black oak at HF, there were no differences between nitrogen treatments in  $\alpha_{\text{FULL}}$  (Fig. 1d, e),  $\tau_{\text{FULL}}$ ,  $\alpha_{\text{nir}}$ ,  $\tau_{\text{nir}}$ ,  $\alpha_{\text{midir}}$ ,  $\tau_{\text{midir}}$ , or FULL absorption [ $1 - (\alpha + \tau)$ ] ( $P > 0.1$  in all cases). For the sweetgum at ORNL, there were no differences between treatments in  $\alpha_{\text{FULL}}$  (except for higher mean values in the ORNL elevated  $\text{CO}_2$  treatment than ORNL N-fertilized treatment; Fig. 1f),  $\tau_{\text{FULL}}$ ,  $\alpha_{\text{nir}}$ , or FULL absorption ( $P > 0.1$  in all cases). There was higher  $\tau_{\text{nir}}$  in the ORNL N-fertilized treatment than in the ambient or elevated  $\text{CO}_2$  treatments ( $P < 0.01$ ). Both  $\alpha_{\text{midir}}$  and  $\tau_{\text{midir}}$  were higher for N-fertilized sweetgums ( $P < 0.01$ ), likely due to differences in LMA and EWT. For all species,  $\alpha_{\text{vis}}$  and  $\tau_{\text{vis}}$  followed differences in N between treatments, with lower values corresponding to higher N fertilization ( $P < 0.05$  in all cases). There was no difference in LMA between nitrogen treatments for black oak or red maple ( $P > 0.1$ ; Fig. 1g, h). However, the N-fertilized treatment at ORNL had lower LMA than the ambient or elevated  $\text{CO}_2$  treatments ( $P < 0.001$ ; Fig. 1i). EWT did not differ between treatments for any species ( $P > 0.1$ ).

### Relationships between N and leaf optical properties

The relationships between  $N_{\text{mass}}$  or  $N_{\text{area}}$  and the  $\alpha$  and  $\tau$  of all optical regions were qualitatively similar across sites and treatments, although  $N_{\text{area}}$  explained less of the variance in foliar optical properties than did  $N_{\text{mass}}$  (Table 1). Variation in  $N_{\text{area}}$  can be caused by changes in LMA or  $N_{\text{mass}}$ , although  $N_{\text{mass}}$  and LMA generally exhibited opposite trends (e.g., LMA is positively correlated with  $\alpha_{\text{vis}}$ , while the relationship between  $N_{\text{mass}}$  and  $\alpha_{\text{vis}}$  is negative). Thus, it

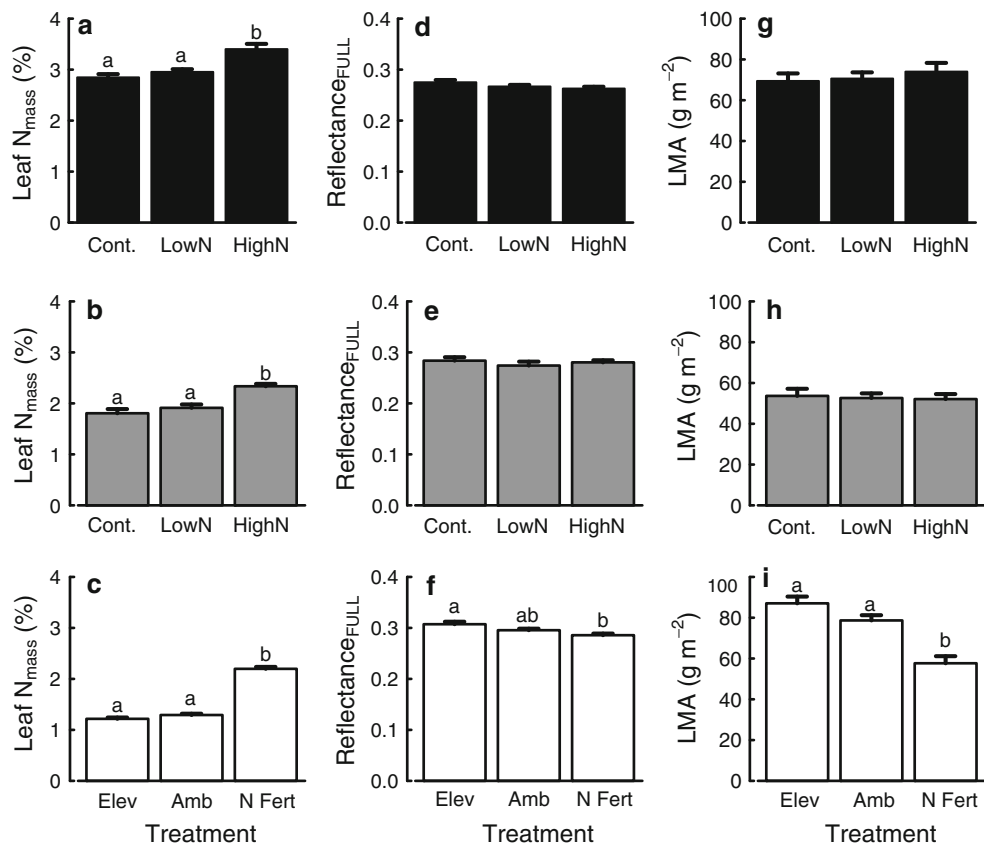


**Fig. 1** ANOVA results (means  $\pm$  standard error) for  $N_{\text{mass}}$  (a–c), solar weighted full spectrum reflectance ( $\alpha_{\text{FULL}}$ ; d–f), and LMA (g m<sup>-2</sup>) treatment differences. Results for black oak (site: HF) are depicted with black

bars, red maple (site: HF) in gray bars, and sweetgum (site: ORNL) in white bars. Means with different letters were significantly different in pair-wise comparisons (Tukey's multiple comparison test)

**Table 1** Comparison of regression statistics for spectrally weighted reflectance and transmittance foliar N on a mass ( $N_{\text{mass}}$ , %) and area basis ( $N_{\text{area}}$ , g m<sup>-2</sup>), reporting the coefficient of determination ( $r^2$ ),  $P$  value, and the sign of the slope of the regression line ('Sign' column) for each model

Response variable	Source of variation					
	$r^2$		$r^2$			
	$N_{\text{mass}}$	$N_{\text{area}}$	$P$ value	Sign	$P$ value	Sign
FULL reflectance	0.26	<0.001	—	—	0.15	<0.001
FULL transmittance		ns				ns
NIR reflectance	0.17	<0.001	—	—	0.06	<0.01
NIR transmittance	0.10	<0.001	+	+	0.05	<0.01
Mid IR reflectance		ns			0.09	<0.001
Mid IR transmittance	0.21	<0.001	+	+		ns
VIS reflectance	0.51	<0.001	—	—	0.17	<0.001
VIS transmittance	0.45	<0.001	—	—	0.31	<0.001

Reflectance and transmittance values are all weighted by the solar spectrum

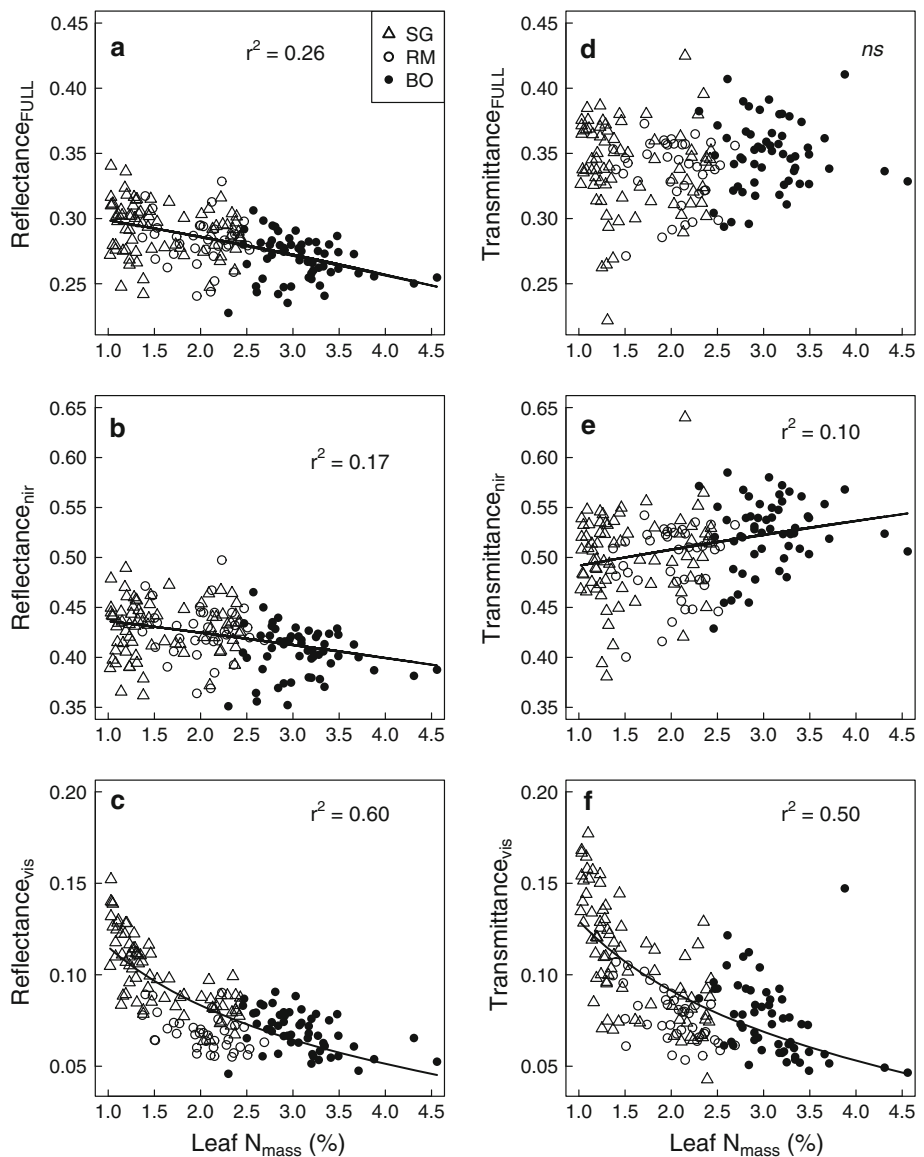
ns insignificant trends

is likely that the similarities between the  $N_{\text{mass}}$  and  $N_{\text{area}}$  relationships are driven by changes in  $N_{\text{mass}}$ , but dampened by the opposing effects of LMA. Because the changes in

$N_{\text{area}}$  can be accounted for by these two variables, subsequent analysis and discussion of foliar N and optical properties will focus on  $N_{\text{mass}}$ . Furthermore,  $N_{\text{mass}}$  was not related to canopy position (height from which foliage was sampled) for any of the species or treatments in our analysis ( $P > 0.1$  in all cases), except for a weak, negative correlation in the elevated sweetgum treatment ( $r^2 = 0.19$ ,  $P < 0.05$ ). As a result, we used mean values from all heights within a tree for subsequent analyses involving  $N_{\text{mass}}$ .

Across all species,  $N_{\text{mass}}$  was the best predictor of FULL, NIR, and visible  $\alpha$  and  $\tau$  for all species combined (Fig. 2), with the exception of  $\tau_{\text{FULL}}$ , which was not correlated with  $N_{\text{mass}}$  ( $P > 0.05$ ). However, contrary to our expectations, the relationships between  $N_{\text{mass}}$  and  $\alpha$  were negative (Fig. 2a–c;  $P < 0.001$  in all cases). There was a positive relationship between both  $\tau_{\text{FULL}}$  and  $\tau_{\text{nir}}$  and  $N_{\text{mass}}$ , whereas the relationship between  $N_{\text{mass}}$  and  $\tau_{\text{vis}}$  was negative (Fig. 2d–f;  $P < 0.001$  in all cases). The relationships between  $N_{\text{mass}}$  and  $\alpha$  in the FULL and NIR regions are primarily due to differences between species [within species, these relationships were not significant ( $P > 0.1$ )], with the exception of sweetgum  $\alpha_{\text{FULL}}$  which showed a slight negative relationship with  $N_{\text{mass}}$  ( $P < 0.05$ ,  $r^2 = 0.06$ ), whereas the relationships

**Fig. 2** Regression between foliar  $N_{\text{mass}}$  and **a** solar-weighted full spectrum reflectance ( $\alpha_{\text{FULL}}$ ; 400–2,500 nm), **b** solar-weighted NIR reflectance ( $\alpha_{\text{nir}}$ ; 700–1,300 nm), and **c** solar-weighted visible reflectance ( $\alpha_{\text{vis}}$ ; 400–700 nm; data log-transformed), **d** solar-weighted full spectrum transmittance ( $\tau_{\text{FULL}}$ ), **e** solar-weighted NIR transmittance ( $\tau_{\text{nir}}$ ), and **f** solar-weighted visible transmittance ( $\tau_{\text{vis}}$ ; data log-transformed). The nonlinear relationship between  $N_{\text{mass}}$  and both  $\alpha_{\text{vis}}$  and  $\tau_{\text{vis}}$  appears to be due to differences in slope between species that vary in their N concentrations. All correlations are significant at  $P < 0.001$ . Black oak (BO), red maple (RM) and sweetgum (SG) were all included in the regression analysis



between  $N_{\text{mass}}$  and the visible region are significant even within species ( $P < 0.05$  in all cases).

Although  $N_{\text{mass}}$  was not a good predictor of  $\alpha_{\text{midir}}$  or  $\tau_{\text{midir}}$ , the relationship was significant and positive for  $\tau_{\text{midir}}$  ( $r^2 = 0.21$ ,  $P < 0.001$ ). There was no relationship between  $N_{\text{mass}}$  and  $\alpha_{\text{midir}}$  ( $P > 0.1$ ). Absorption was positively correlated with  $N_{\text{mass}}$  in the visible ( $r^2 = 0.52$ ,  $P < 0.001$ ) and the Mid IR ( $r^2 = 0.17$ ,  $P < 0.001$ ), but not in the NIR ( $P > 0.1$ ), leading to a weak, positive relationship between total FULL absorption and  $N_{\text{mass}}$  ( $r^2 = 0.07$ ,  $P < 0.01$ ). There was some colinearity between spectral response variables, which is not surprising, as they are all part of the same overall spectra. However, the different regions responded differently, because absorbers are located primarily in the visible (pigment absorption) and Mid IR (water absorption), with the NIR being primarily influenced by scattering (Ollinger 2011).

The above results describe how  $N_{\text{mass}}$  varied with  $\alpha$  and  $\tau$  for a single leaf. In leaf stacks, the correlation coefficients for the relationships between  $N_{\text{mass}}$  and foliar optical properties decreased as the number of leaves increased. Despite this, the negative slopes of the relationship between  $N_{\text{mass}}$  and  $\alpha_{\text{FULL}}$  remained intact for all leaf stacks (Fig. 3;  $P < 0.001$  in all cases).

#### Relationships between leaf traits and leaf optical properties

Across all species and treatments, there was a weak, positive correlation between LMA and  $\alpha_{\text{FULL}}$  ( $P < 0.05$ ), and weak, negative correlation between LMA and both  $\tau_{\text{FULL}}$  and  $\tau_{\text{nir}}$  (Fig. 4;  $P < 0.001$  in both cases). There were stronger negative correlations between LMA and  $\alpha_{\text{midir}}$  ( $r^2 = 0.38$ ,  $P < 0.001$ ) and  $\tau_{\text{midir}}$  ( $r^2 = 0.40$ ,  $P < 0.001$ ), although this is likely due to the influence of EWT. LMA was positively cor-

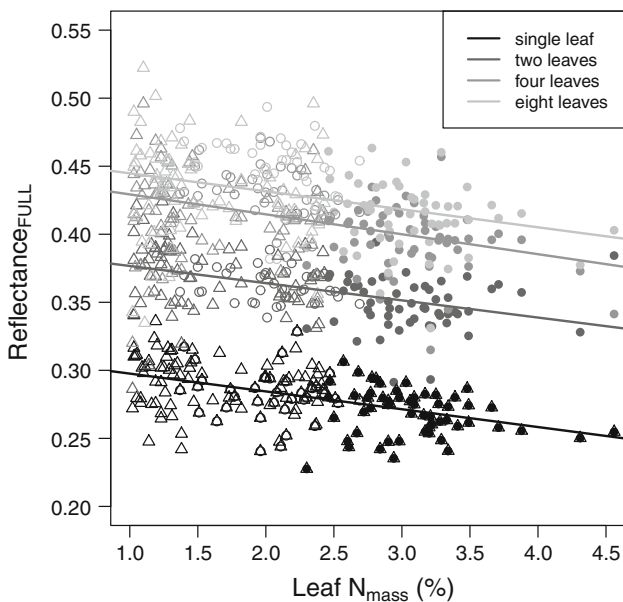


**Fig. 3** Foliar  $N_{\text{mass}}$  versus solar weighted full spectrum reflectance ( $\alpha_{\text{FULL}}$ ) for stacks of one ( $r^2 = 0.25, P < 0.001$ ), two ( $r^2 = 0.18, P < 0.001$ ), four ( $r^2 = 0.15, P < 0.001$ ), and eight ( $r^2 = 0.10, P < 0.001$ ) leaves. Black oak (*BO*), red maple (*RM*) and sweetgum (*SG*) were all included in the regression analysis. Although the y-intercept differs, all stacks show similar negative relationships between foliar N and  $\alpha_{\text{FULL}}$

related with  $\alpha_{\text{vis}}$  ( $r^2 = 0.20, P < 0.001$ ), whereas there was no relationship between  $\tau_{\text{vis}}$  and LMA ( $P > 0.1$ ).

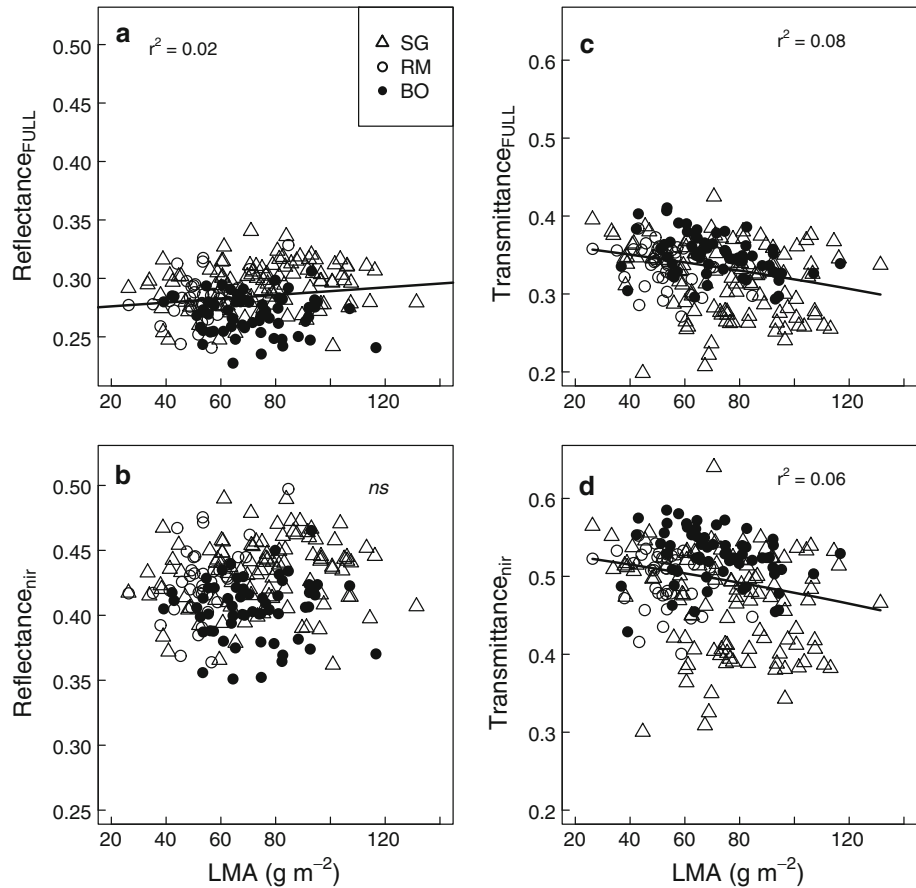
Equivalent water thickness was negatively correlated with  $\alpha_{\text{midir}}$  and  $\tau_{\text{midir}}$  and was the best overall predictor of Mid IR foliar optical properties (Fig. 5;  $P < 0.001$  in all cases). EWT was weakly, but positively, correlated with  $\alpha_{\text{FULL}}$  ( $r^2 = 0.06, P < 0.01$ ),  $\alpha_{\text{nir}}$  ( $r^2 = 0.04, P < 0.01$ ), and  $\alpha_{\text{vis}}$  ( $r^2 = 0.28, P < 0.001$ ), and negatively correlated with  $\tau_{\text{FULL}}$  ( $r^2 = 0.10, P < 0.001$ ) and  $\tau_{\text{nir}}$  ( $r^2 = 0.09, P < 0.001$ ). Relative water content ( $\text{g H}_2\text{O g}^{-1}$  fresh leaf tissue) was not correlated with any foliar optical parameter we considered ( $P > 0.1$  in all cases).

Multiple regression models using all combinations of leaf traits did not improve predictions for  $\alpha_{\text{FULL}}$ ,  $\tau_{\text{FULL}}$ ,  $\alpha_{\text{nir}}$ , or  $\tau_{\text{nir}}$  above that which was obtained by  $N_{\text{mass}}$  alone.

#### Relationships between leaf traits

The relationship between LMA and EWT was significant and positive both within (black oak:  $r^2 = 0.73$ ; red maple:  $r^2 = 0.36$ ; sweetgum:  $r^2 = 0.46$ ;  $P < 0.001$  in all cases) and across ( $r^2 = 0.54, P < 0.001$ ) all species. LMA and  $N_{\text{mass}}$  were negatively correlated within sweetgums ( $r^2 = 0.22$ ,

**Fig. 4** Regression between LMA and **a** solar-weighted full spectrum reflectance ( $\alpha_{\text{FULL}}$ ;  $P < 0.05$ ), **b** solar-weighted NIR reflectance ( $\alpha_{\text{nir}}$ ;  $P > 0.1$ ), **c** solar-weighted full spectrum transmittance ( $\tau_{\text{FULL}}$ ;  $P < 0.001$ ), and **d** solar-weighted NIR transmittance ( $\tau_{\text{nir}}$ ;  $P < 0.001$ ). Black oak (*BO*), red maple (*RM*) and sweetgum (*SG*) were all included in the regression analysis



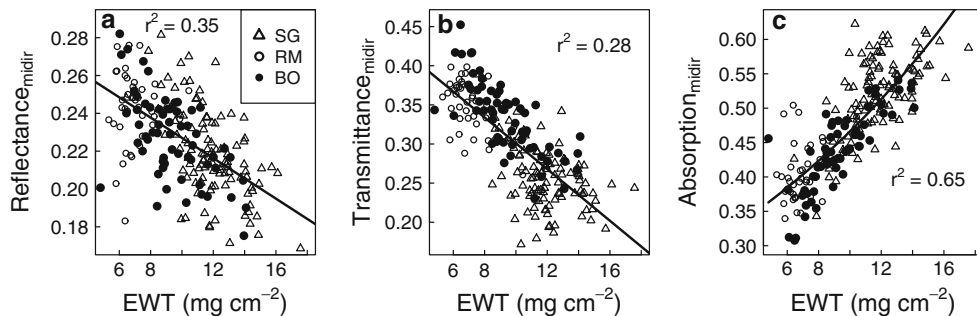


**Fig. 5** Both **a** solar-weighted reflectance ( $\alpha$ ) and **b** solar-weighted transmittance ( $\tau$ ) declined in the Mid IR region (700–1,350 nm) as leaf EWT increased. This was due to the strong positive correlation between Mid IR absorption [ $1 - (\alpha + \tau)$ ] and EWT (**c**), which demon-

strates the importance of water absorption in the Mid IR in influencing scattering from this region. All correlations are significant at  $P < 0.001$ . Black oak (*BO*), red maple (*RM*) and sweetgum (*SG*) were all included in the regression analysis

$P < 0.001$ ), but the relationship was not significant in black oaks, red maples, or across all species. EWT and  $N_{\text{mass}}$  were not significantly correlated within any species ( $P > 0.1$  in all cases), but with all species combined they were slightly negatively related ( $r^2 = 0.05$ ,  $P < 0.01$ ).

#### Canopy-level reflectance

Despite the absence of differences in leaf-level reflectance between treatments, reflectance data obtained from the AVIRIS sensor showed that whole-canopy NIR reflectance was higher for the N-fertilized sweetgum treatment than the ambient CO<sub>2</sub> sweetgum treatment (Fig. 6;  $P < 0.001$ ). Canopy NIR reflectance from the elevated CO<sub>2</sub> sweetgum treatment was lower than the ambient CO<sub>2</sub> sweetgum treatment, although the trend was not significant (Fig. 6;  $P > 0.1$ ) and the difference was small compared to that between the N-fertilized and ambient CO<sub>2</sub> treatments. There was little to

no difference in canopy reflectance in the visible or MIR portions of the spectrum.

#### Discussion

A primary goal of this study was to examine relationships between leaf traits and leaf optical properties that might help explain the positive correlation between canopy  $N_{\text{mass}}$  and full spectrum canopy albedo seen in temperate and boreal forests (Ollinger et al. 2008; Hollinger et al. 2010). Our results do not support the hypothesis that the canopy-level trend was caused by a similar trend occurring at the leaf level. There were no differences in leaf  $\alpha_{\text{FULL}}$  or  $\tau_{\text{FULL}}$  between comparable N or CO<sub>2</sub> treatments, despite changes in leaf  $N_{\text{mass}}$  caused by N fertilization and increases in whole canopy NIR reflectance, as measured using AVIRIS, in the N-fertilized plots at ORNL. Earlier work showed a reduction in leaf  $N_{\text{mass}}$  in CO<sub>2</sub>-treated plots relative to controls at ORNL (Norby and Iversen 2006). Although we also saw lower  $N_{\text{mass}}$  in CO<sub>2</sub>-treated plots, the difference was smaller and not significant. As a result, our prediction that foliar  $\alpha$  would decrease with increased CO<sub>2</sub> fertilization was neither supported nor refuted.

Whereas the slope of the previously observed relationship between  $N_{\text{mass}}$  and canopy full spectrum albedo is positive, we observed a negative relationship at the leaf level, when all species and treatments were combined. This pattern was driven in part by the visible region, where high N foliage is expected to absorb more light due to increased pigment concentration. Nevertheless, the relationship was also negative, albeit weaker, even when restricted to the NIR region.

To what can we attribute these results? Previous studies have linked scattering and NIR reflectance to leaf structural parameters such as leaf thickness, percent intercellular air space (%IAS), or the  $A_{\text{mes}}/A$  ratio (Knapp and Carter 1998; Gausman et al. 1970; Slaton et al. 2001). In our own data,

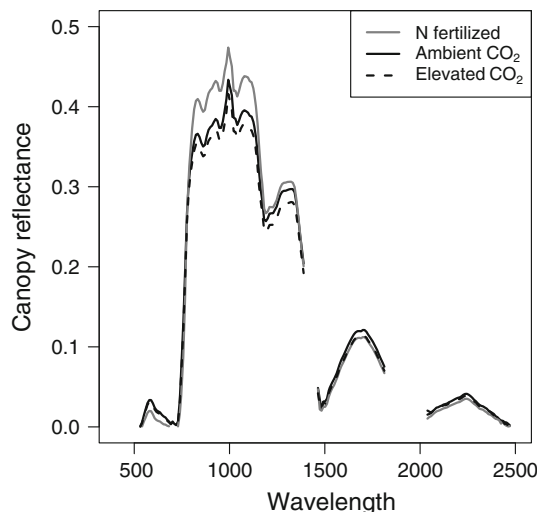


**Fig. 6** AVIRIS canopy reflectance across the full spectrum for N-fertilized, ambient CO<sub>2</sub>, and elevated CO<sub>2</sub> sweetgum treatments at ORNL

there was no correlation between  $\alpha_{\text{nir}}$  and LMA, although this could be due to the confounding effects on reflectance of leaf thickness and leaf density, two variables that determine LMA, but have opposing effects on other leaf traits such as the fraction of leaf volume composed of intercellular air space (increased leaf thickness increases %IAS, whereas increased leaf density decreases %IAS; Niinemets 1999, 2001). A number of studies have observed positive relationships between NIR reflectance and %IAS (Castro-Esau et al. 2006; Gausman et al. 1970; Slaton et al. 2001), while others suggest varying relationships between %IAS and foliar  $N_{\text{mass}}$ . In a study involving fertilization of tall fescue (*Festuca arundinacea* Schreb.), Rademacher and Nelson (2001) found that the ratio of IAS to total mesophyll space was lower in high N foliage because N fertilization enhanced mesophyll area to a greater degree than leaf volume. Conversely, Niinemets (1999), across a broad range of woody vegetation, observed a negative relationship between leaf density and both  $N_{\text{mass}}$  and the fraction of leaf mesophyll as intercellular airspace. This implies that leaves with high foliar N should be less dense and have a greater %IAS.

In contrast to our leaf level results, remote sensing data collected by the AVIRIS sensor showed an increase in whole-canopy NIR reflectance with N fertilization in the ORNL sweetgum plantation, a response that is consistent with observations along natural gradients in plant N status (Ollinger et al. 2008; Hollinger et al. 2010). Collectively, these results suggest that the association between  $N_{\text{mass}}$  and canopy NIR reflectance is driven by stem or canopy level properties that are either influenced by, or covary with, leaf  $N_{\text{mass}}$ .

In our study, the only canopy structural variable we were able to evaluate was leaf area index (LAI, leaf area per unit area of ground), which was higher in the ORNL N-fertilized plots than in the control plots (LAI ~ 5.5 and 4.5, respectively; Richard Norby and Colleen Iversen, personal communication). To evaluate the potential effect of this difference on the canopy reflectance values observed by AVIRIS, we used SAIL-2 (Scattering from Arbitrarily Inclined Leaves; Verhoef 1984; Braswell et al. 1996), a radiative transfer model that has been used extensively in the literature (e.g., Huemmrich and Goward 1997; Andrieu et al. 1997; Daughtry et al. 2000; Zhang et al. 2006). Although SAIL is known to be sensitive to changes in LAI, especially in low-LAI systems (e.g., Asner 1998), model runs for the control and N-fertilized plots, conducted using measured LAI and measured leaf and background reflectance and transmittance spectra, produced a negligible difference in canopy reflectance (Fig. 7). This suggests that canopy properties other than LAI are driving the observed changes in canopy reflectance between the stands.

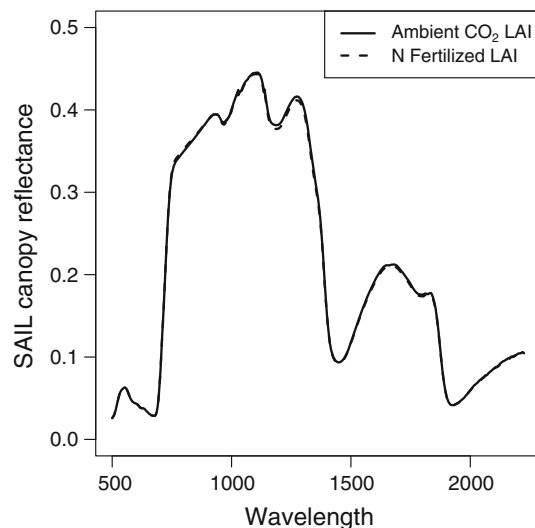


**Fig. 7** Results of SAIL-2 model runs for the ambient CO<sub>2</sub> and N-fertilized plots, conducted using measured LAI and measured leaf and background reflectance and transmittance spectra. Resulting spectra show a negligible difference in canopy reflectance

Other canopy properties that may provide a link between plant N status and canopy reflectance include shoot architecture (Smolander and Stenberg 2003; Malenovský et al. 2008), crown geometry (e.g., Rautiainen et al. 2004)- and leaf angle distribution (Asner 1998; Close and Beadle 2006). Each of these are influenced by a variety of resource optimization mechanisms that are known to vary with plant nutrient status, perhaps resulting in associations between leaf traits and canopy structural properties that have yet to be explored (e.g., Ollinger 2011). As an example, N fertilization experiments involving eucalyptus (Close and Beadle 2006), wheat (Brooks et al. 2000)- and rice (Tari et al. 2009) have all demonstrated reductions in mean leaf angle (i.e.- leaves become more horizontal) with improved N nutrition. Because low leaf angle is associated with increased reflectance, particularly in the NIR region (Asner 1998; Ollinger 2011), such a response could contribute to a positive relationship between  $N_{\text{mass}}$  and canopy albedo if it were to occur over broad gradients within native ecosystems. Canopy leaf angle is a challenging parameter to measure, and at present, we lack the data needed to evaluate the extent to which variation in leaf angle, or other related parameters, may have contributed to our results.

## Conclusions

This study investigated the importance of leaf-level reflectance properties as a potential cause of the relationship between foliar  $N_{\text{mass}}$  and canopy full spectrum albedo. Although we cannot completely rule out the importance of mechanisms involving leaf-level radiation scattering, our

results suggest that they are not the dominant influence on this relationship. Instead, we suggest that the principal mechanism lies in associations between leaf-level  $N_{\text{mass}}$  and optically important canopy structural properties that have yet to be thoroughly explored. Although measuring canopy structural properties is challenging, future work should consider variables such as leaf arrangement and foliage clumping, leaf angle distribution, and crown geometry, in conjunction with leaf traits and canopy spectral properties. If met with success, such investigations would improve our overall understanding of how biogeochemical processes influence biophysical properties that are relevant to surface energy exchange and interactions between ecosystems and climate.

**Acknowledgments** We thank G. James Collatz for helpful comments on a draft of this manuscript, Rob Braswell for providing the SAIL-2 model code, and Richard Norby, Colleen Iversen, and Jeffery Warren for support at ORNL. We are indebted to Michael Eastwood, ER-2 pilots Denis Steel, Tim Williams, and the rest of the AVIRIS team for aircraft data acquisition. This work was funded by a grant from the North American Carbon Program (NACP) NASA's Terrestrial Ecology and Carbon Cycle Science Programs and a graduate fellowship provided by the Research and Discover program. The ORNL FACE experiment was supported by the US Department of Energy, Office of Science, Biological and Environmental Research Program. A.D.R. and M.K.B. acknowledge support, through the Harvard Forest REU program, from the National Science Foundation (Grant DBI-04-52254).

## References

- Andrieu B, Baret F, Jacquemoud S, Malthus T, Steven M (1997) Evaluation of an improved version of SAIL model for simulating bidirectional reflectance of sugar beet canopies. *Remote Sens Environ* 60:247–257
- Asner GP (1998) Biophysical and biochemical sources of variability in canopy reflectance. *Remote Sens Environ* 64:234–253
- Braswell BH, Schimel DS, Privette JL, Moore B III, Emery WJ, Sulzman EW, Hudak AT (1996) Extracting ecological and biophysical information from AVHRR optical data: an integrated algorithm based on inverse modeling. *J Geophys Res* 101:23335–23348
- Brooks TJ, Wall GW, Pinter PJ Jr, Kimball BA, LaMorte RL, Leavitt SW, Matthias AD, Adamsen FJ, Hunsaker DJ, Webber AN (2000) Acclimation response of spring wheat in a free-air  $\text{CO}_2$  enrichment (FACE) atmosphere with variable soil nitrogen regimes. 3. Canopy architecture and gas exchange. *Photosynth Res* 66:97–108
- Castro-Esau KL, Sanchez-Azofeifa GA, Rivard B, Wright AJ, Quesada M (2006) Variability in leaf optical properties of Mesoamerican trees and the potential for species classification. *Am J Bot* 94:517–530
- Chen JM, Cihlar J (1995) Quantifying the effect of canopy architecture on optical measurements of leaf area index using two gap size analysis methods. *IEEE Transact Geosci Remote Sens* 33:777–787
- Close DC, Beadle CL (2006) Leaf angle responds to nitrogen supply in eucalypt seedlings. Is it a photoprotective mechanism? *Tree Physiol* 26:743–748
- Daughtry CST, Walthall CL, Kim MS, Brown de Colstoun E, McMurry JE III (2000) Estimating corn leaf chlorophyll concentration from leaf and canopy reflectance. *Remote Sens Environ* 74:229–239
- Ellsworth DS, Reich PB, Naumburg ES, Koch GW, Kubiske ME, Smith SD (2004) Photosynthesis, carboxylation and leaf nitrogen responses of 16 species to elevated  $\text{pCO}_2$  across four free-air  $\text{CO}_2$  enrichment experiments in forest, grassland and desert. *Glob Change Biol* 10:2121–2138
- Evans JR (1989) Photosynthesis and nitrogen relationships in leaves of C3 plants. *Oecologia* 78:9–19
- Field C, Mooney HA (1986) The photosynthesis-nitrogen relationship in wild plants. In: Givnish TI (ed) On the economy of form and function. Cambridge University Press, Cambridge, pp 25–55
- Gates DM, Keegan HJ, Schleter JC, Weidner VR (1965) Spectral properties of plants. *Appl Opt* 4:11–20
- Gausman HW, Allen WA, Cardenas R, Richardson AJ (1970) Relation of light reflectance to historical and physical evaluations of cotton leaf maturity. *Appl Opt* 9:545–552
- Gausman HW, Allen WA, Escobar DE (1974) Refractive index of plant cell walls. *Appl Opt* 13:109–111
- Guemard C (2004) The sun's total and spectral irradiance for solar energy applications and solar radiation models. *Sol Energy* 76:423–453
- Hollinger DY, Ollinger SV, Richardson AD, Meyers TP, Dail DB, Martin ME, Scott NA, Arkebauer TJ, Baldocchi DD, Clark KL, Curtis PS, Davis KJ, Desai AR, Dragoni D, Goulden ML, Gu L, Katul GG, Pallardy SG, Paw UKT, Schmid HP, Stoy PC, Suyker AE, Verma SB (2010) Albedo estimates for land surface models and support for a new paradigm based on foliage nitrogen concentration. *Glob Change Biol* 16:696–710
- Huemmrich KF, Goward SN (1997) Vegetation canopy PAR absorptance and NDVI: an assessment for ten tree species with the SAIL model. *Remote Sens Environ* 61:254–269
- Iversen CM, Norby RJ (2008) Nitrogen limitation in a sweetgum plantation: implications for carbon allocation and storage. *Can J For Res* 38:1021–1032
- Jacquemoud S, Verhoef W, Baret F, Bacour C, Zarco-Tejada PJ, Asner GP, François C, Ustin SL (2009) PROSPECT + SAIL models: a review of use for vegetation characterization. *Remote Sens Environ* 113:S56–S66
- Johnson DW, Cheng W, Joslin JD, Norby RJ, Edwards NT, Todd DE Jr (2004) Effects of elevated  $\text{CO}_2$  on nutrient cycling in a sweetgum plantation. *Biogeochemistry* 69:379–403
- Knapp AK, Carter GA (1998) Variability in leaf optical properties among 26 species from a broad range of habitats. *Am J Bot* 85:940–946
- Longstreth DJ, Bolaños JA, Goddard RH (1985) Photosynthetic rate and mesophyll surface area in expanding leaves of *Alternanthera philoxeroides* grown at two light levels. *Am J Bot* 72:14–19
- Magill AH, Aber JD, Currie WS, Nadelhoffer KJ, Martin ME, McDowell WH, Melillo JM, Steudler P (2004) Ecosystem response to 15 years of chronic nitrogen additions at the Harvard Forest LTER, Massachusetts, USA. *For Ecol Manag* 196:7–28
- Malenovský Z, Martin E, Homolová L, Gastellu-Etchegorry J-P, Zurieta-Milla R, Schaeppman ME, Pokorný R, Clevers JGPW, Cudlín P (2008) Influence of woody elements of a Norway spruce canopy on nadir reflectance simulated by the DART model at very high spatial resolution. *Remote Sens Environ* 112:1–18
- Niinemets U (1999) Research review: components of leaf dry mass per area-thickness and density-alter leaf photosynthetic capacity in reverse directions in woody plants. *New Phytol* 144:35–47
- Niinemets U (2001) Global-scale climatic controls of leaf dry mass per area, density, and thickness in trees and shrubs. *Ecology* 82:453–469

- Nobel PS, Zaragoza LJ, Smith WK (1975) Relation between mesophyll surface area, photosynthetic rate, and illumination level during development for leaves of *Plectranthus parviflorus* Henckel. *Plant Physiol* 55:1067–1070
- Norby RJ, Iversen CM (2006) Nitrogen uptake, distribution, turnover, and efficiency of use in a CO<sub>2</sub>-enriched sweetgum forest. *Ecology* 87:5–14
- Norby RJ, Todd DE, Fults J, Johnson DW (2001) Allometric determination of tree growth in a CO<sub>2</sub>-enriched sweetgum stand. *New Phytol* 150:477–487
- Norby RJ, Sholtis JD, Gunderson CA, Jawdy SS (2003) Leaf dynamics of a deciduous forest canopy: no response to elevated CO<sub>2</sub>. *Oecologia* 136:574–584
- Ollinger SV (2011) Sources of variability in canopy reflectance and the convergent properties of plants. *New Phytol* 189:375–394
- Ollinger SV, Aber JD, Lovett GM, Millham SE, Lathrop RG, Ellis JE (1993) A spatial model of atmospheric deposition for the Northeastern US. *Ecol Appl* 3:459–472
- Ollinger SV, Richardson AD, Martin ME, Hollinger DY, Frolking S, Reich PB, Plourde LC, Katul GG, Munger JW, Oren R, Smith ML, Paw UKT, Bolstad PV, Cook BD, Day MC, Martin TA, Monson RK, Schmid HP (2008) Canopy nitrogen, carbon assimilation and albedo in temperate and boreal forests: functional relations and potential climate feedbacks. *Proc Nat Acad Sci* 105:19335–19340
- Oren R, Ellsworth DS, Johnsen KH, Phillips N, Ewers BE, Maier C, Schäfer KVR, McCarthy H, Hendrey G, McNulty SG, Katul GG (2001) Soil fertility limits carbon sequestration by forest ecosystems in a CO<sub>2</sub>-enriched atmosphere. *Nature* 411:469–472
- Rademacher IF, Nelson CJ (2001) Nitrogen effects on leaf anatomy within the intercalary meristems of tall fescue leaf blades. *Ann Bot* 88:893–903
- Rautiainen M, Stenberg P, Nilson T, Kuusk A (2004) The effect of crown shape on the reflectance of coniferous stands. *Remote Sens Environ* 89:41–52
- Reich PB, Walters MB, Ellsworth DS (1997) From tropics to tundra: global convergence in plant functioning. *Proc Nat Acad Sci* 94:13730–13734
- Reich PB, Ellsworth DS, Walters MB, Vose JM, Gresham C, Volin JC, Bowman WD (1999) Generality of leaf train relationships: a test across six biomes. *Ecology* 80:1955–1969
- Riggs JS, Tharp ML, Norby RJ (2009) ORNL FACE CO<sub>2</sub> data. carbon dioxide information analysis center, Oak Ridge, TN, USA. <http://cdiac.ornl.gov>. Accessed 15-July-2010
- Sánchez J, Canton MP (1999) Space imaging processing. CRC Press LLC, Boca Raton
- Slaton MR, Hunt ER, Smith WK (2001) Estimating near-infrared leaf reflectance from leaf structural characteristics. *Am J Bot* 88:278–284
- Smolander S, Stenberg P (2003) A method to account for shoot scale clumping in coniferous canopy reflectance models. *Remote Sens Environ* 88:363–373
- Tari DB, Gazanchian A, Pirdashti HA, Nasiri M (2009) Flag leaf morphophysiological response to different agronomical treatments in a promising line of rice (*Oryza sativa* L.). *Am-Euras J Agric Environ Sci* 5:403–408
- Verhoef W (1984) Light scattering by leaf layers with application to canopy reflectance modeling: the SAIL model. *Remote Sens Environ* 16:125–141
- Woolley JT (1971) Reflectance and transmittance of light by leaves. *Plant Physiol* 47:656–662
- Wright IJ, Reich PB, Westoby M, Ackerly DD, Baruch Z, Bongers F, Cavender-Bares J, Chapin T, Cornelissen JHC, Diemer M, Flexas J, Garnier E, Groom PK, Gulias J, Hikosaka K, Lamont BB, Lee T, Lee W, Lusk C, Midgley JJ, Navas M-L, Niinemets U, Oleksyn J, Osada N, Poorter H, Poot P, Prior L, Pyankov VI, Roumet C, Thomas SC, Tjoelker MG, Veneklaas EJ, Villar R (2004) The worldwide leaf economics spectrum. *Nature* 428:821–827
- Zhang Q, Xiao X, Braswell BH, Linder E, Ollinger S, Smith ML, Jenkins JP, Baret F, Richardson AD, Moore B III, Minocha R (2006) Characterization of seasonal variation of forest canopy in a temperate deciduous broadleaf forest, using daily MODIS data. *Remote Sens Environ* 105:189–203